

The Distribution of Vacua in Random Landscape Potentials

Low Lerh Feng, Shaun Hotchkiss and Richard Easther

Department of Physics,
University of Auckland,
Private Bag 92019,
Auckland, New Zealand

E-mail: lerh.low@auckland.ac.nz, s.hotchkiss@auckland.ac.nz,
r.easther@auckland.ac.nz

Abstract. Landscape cosmology posits the existence of a convoluted, multidimensional, scalar potential – the “landscape” – with vast numbers of metastable minima. The huge number of minima supported by landscape potentials motivate arguments that landscape cosmology reduces tuning problems associated with a small but non-zero vacuum energy by providing a framework in which anthropic or “environmental” selection is plausible. Random matrices and random functions in many dimensions can be used to discuss conceptual issues associated with landscape scenarios; here we explore ~~the distribution~~ the minima ~~as a function of~~ and vacuum energy in an N -dimensional Gaussian random potential. We derive a probability density for the density of minima in N dimensions, showing that after rescalings its properties are fully defined by N and a single free parameter. This gives us $P(\Lambda)$, the probability density function of vacuum energies in these scenarios. [RE: little more to come]

Contents

1	Introduction	1
2	Random Potentials in N Dimensions	3
3	Peak Probabilities: V and N	6
3.1	Landscape Heuristics	7
3.2	$N < 10$: Direct Evaluation	8
3.3	$10 < N < \sim 30$: Gaussian Approximations to the Integral	8
3.4	$\sim 30 < N < \sim 100$: Approximations using the $\nu = 0$ point	9
4	Implications for Multiverse Cosmology	10
5	Conclusion	10
6	Appendix	11
6.1	Density of peaks for $N = 4$	11
6.2	$p(F s.p.)$ for $N = 2$	13

1 Introduction

Over the last two decades cosmology has developed in apparently paradoxical directions. Observationally, the rise of “precision cosmology” makes it possible to measure key parameters to within a few percent, setting stringent tests for the detailed evolutionary narrative given by concordance Λ CDM cosmology [1, 2]. Conversely, theoretical investigations of both slow-roll inflation and string theory along with a non-zero dark energy density motivates theoretical investigations of multiverse-like scenarios. In particular, studies of stochastic inflation [3, 4] suggest that the mechanism that produces astrophysical density perturbations could also support *eternal inflation*, generating infinite numbers of *pocket universes* [5]. Likewise, studies of flux compactified string vacua points to a possible *landscape* [6] or *discretuum* [7] of vacua within the theory. These developments open the door to anthropic explanations of the non-zero vacuum energy density, insofar as a value that was exactly zero could have been more plausibly explained by an unknown symmetry.

Stochastic (or eternal) inflation implies the existence of a multiverse composed of many pocket universes, but this does not require that the “low energy” (i.e. LHC scale) physics or vacuum energy differs between pockets: the naive quadratic inflation model is potentially eternal, but has a unique vacuum. By contrast, landscape models have multiple vacua which can, in principle, be populated by stochastic inflation or tunneling. The string landscape, built on the plethora of flux-stabilised vacua that exist inside Calabi-Yau spaces, is well-known but is not necessarily a unique realisation of this scenario. The complexity of the landscape and the vast number of vacua it

supports is the basis of its purported explanatory power: the number of vacua is almost uncountably large (e.g. 10^{500} or greater [42]) and any value of the vacuum energy can thus conceivably be realised within it.

The detailed properties of any possible landscape are almost entirely unknown – it is still unclear whether any specific stringy construction realises the $SU(3) \times SU(2) \times U(1)$ gauge group of the Standard Model. More recently the Swampland Conjecture suggests that all stable minima of the theory might actually be “underwater” [8], located at negative values of Λ . If true, this would require that the cosmological dark energy was underpinned by dynamical quintessence-like evolution.

An alternative approach to landscape scenarios is to strip them down to their barest essence – by realising multiverse cosmology within a *random* multidimensional ($N \sim 100$ or more) potential of interacting scalar fields.¹ In this approach the “large N ” properties of the multidimensional landscape actually provides leverage that can be used to develop an understanding of its properties. The first steps in this direction were taken by Aazami and Easther [12], investigating ensembles of Hessian matrices describing extrema in a random landscape. At a minimum in the landscape the eigenvalues of the Hessian are all positive. For simple random matrix distributions eigenvalues are likely to be evenly distributed between positive and negative values with fluctuations away from this situation being strongly suppressed at even moderate values of N , suggesting that the number of minima is super-exponentially smaller than the number of saddles. However, the individual entries of Hessians matrices of random functions are correlated and therefore not drawn from identical, independent distributions,[32, 35] violating a common premise of **simple** random matrix theory **and making minima more probable**. ~~That said,~~ This overall approach has **now** been widely pursued and has **now** been extended in a number of directions [14–21] This line of inquiry has also motivated studies of the properties of random matrices and random functions at large N . [13, 29–34] Similar mathematical problems arise in statistical mechanics, string theory, and complex dynamics.[22–28]

In the conventional picture of the multiverse, the universe ~~traces out a path~~ exists in a local minimum of the landscape. ~~If it moves along a path where the gradient of the potential is small, there is so-called “slow-roll” inflation. Eventually, the universe’s evolution ends in a minimum of the potential. If this is the global minimum, the end-state is stable. However, bubbles of space can tunnel from a local minimum to lower-lying vacua, rendering local minima metastable, although often with lifetimes much greater than the age of the universe.~~ [SH: Do we need to write the above?] If this local minimum has a positive vacuum energy it will contribute an apparent cosmological constant term to observers within the universe. Accordingly, we are interested in the probability of minima having potential values $V > 0$. ~~In particular,~~ [SH: check] We show that for a region of parameter space, a random potential with 10^M minima (where M is a number of order $\mathcal{O}(100)$) can also have $P(V > 0|\text{min}) \ll 10^{-M}$, so that it is conceivable that these scenarios have no metastable solutions with positive vacuum

¹Random is used here in the context of random function theory [9–11]. We refer to random functions rather than random fields, the nomenclature often seen in the mathematical literature, to avoid confusion with the individual scalar fields that are coupled by the potential.

energy.

These considerations may lead to a weakly non-uniform measure on the vacuum energy [\[RE: more on measure problem, including definition and citations\]](#)

Finally, the methods we use also provide a probability density for the eigenvalues at minima, allowing us to infer the shape [around the minima \[RE: more to come\]](#)

We start [by generalising to \$N\$ dimensions](#) the Kac-Rice formalism [\[36, 37\]](#) and the machinery developed [and summarised](#) by Bond, Bardeen, Kaiser and Szalay [\[38\]](#) for studying the statistics of Gaussian random functions ~~–cosmological-perturbation theory to N dimensions~~. This yields N -dimensional integral expressions for ~~all terms of interest~~ the proportion of minima that will have a given value of the potential, V . At $N = 2$ the full integral can be evaluated analytically; at $N \lesssim 10$ we can ~~directly~~ numerically compute the full integrals; and for $N \lesssim 100$ ~~then to numerical evaluations of~~ we evaluate Gaussian approximations to the underlying integrals ~~out to $N = 100$~~ . The Gaussian approximations are tested against the exact numerical result for $N < 10$ where they match closely. These techniques can be generalised to other, more complex questions about trajectories in these potentials, and give information about the “shapes” of minima which may inform analyses of tunnelling and inflation. We show that $P(\Lambda)$, the probability density function for the vacuum energy, depends on the dimensionality N and a single free parameter for a Gaussian random landscape, and calculate how $P(\Lambda)$ varies with N . Finally, we discuss the implications of these results for landscape cosmology and notions of anthropic selection. [\[RE: more detail here\]](#)[\[SH: we still use \$V\$ and \$\Lambda\$ interchangeably in the paper, without much apparent order. I would favour only using \$\Lambda\$ very sparingly when explicitly referring to the observed vacuum energy. Or, perhaps \$\Lambda\$ is only ever the value of \$V\$ when it is explicitly in a minimum?\]](#)

2 Random Potentials in N Dimensions

We treat the potential energy function $V(\vec{\phi})$ as a Gaussian random function over an N -dimensional field space. We wish to examine minima and saddles, therefore we require the probability density for the value of the potential itself and the values of its derivatives, $\eta_i = \partial V / \partial \phi^i$ and $\zeta_{ij} = \partial^2 V / \partial \phi^i \partial \phi^j$ at individual points in this field space. These variables can be grouped together into a vector $\mathbf{y} = [V, \eta, \zeta]$. In N dimensions \mathbf{y} has $\mathcal{N} = 1 + N + (N^2 + N)/2$ independent components via V , η and ζ respectively. V is a Gaussian random function, this means that the variables in \mathbf{y} are described by a multivariate Gaussian distribution. A general multivariate Gaussian distribution with \mathcal{N} independent variables has the form

$$P(\mathbf{y}) d^{\mathcal{N}} \mathbf{y} = \frac{e^{-Q}}{[(2\pi)^{\mathcal{N}} \det(M)]^{1/2}} d^{\mathcal{N}} \mathbf{y}, \quad (2.1)$$

$$Q \equiv \frac{1}{2} \sum_{i,j}^{\mathcal{N}} \Delta y_i (M^{-1})_{ij} \Delta y_j.$$

Here Δy_i is the difference between the actual value and the mean value, i.e. $\Delta y_i \equiv y_i - \langle y_i \rangle$, and M is the *covariance matrix*,

$$M_{ij} \equiv \langle \Delta y_i \Delta y_j \rangle. \quad (2.2)$$

Averages denoted by $\langle \rangle$ are ensemble averages. We further assume that $\langle V \rangle = \langle \eta \rangle = \langle \zeta \rangle = 0$.² Therefore the probability density only depends on the covariance matrix, M , and its inverse.

We next introduce the field space power spectrum, P , of the random function V , which will be useful for writing M in a concise form. We define it here to be the Fourier transform of the correlation function of V , i.e.

$$\langle V(\vec{\phi}_1) V(\vec{\phi}_2) \rangle = \xi(|\vec{\phi}_1 - \vec{\phi}_2|) = \frac{1}{(2\pi)^N} \int d^N k e^{i\vec{k} \cdot (\vec{\phi}_1 - \vec{\phi}_2)} P(k). \quad (2.3)$$

We have assumed V is statistically homogeneous and isotropic in field space, therefore ξ depends only on $|\vec{\phi}_1 - \vec{\phi}_2|$ and P depends only on the magnitude of the Fourier coordinate k .³ The moments of the power spectrum can be defined as

$$\sigma_n^2 = \frac{1}{(2\pi)^N} \int d^N k (k^2)^n P(k) \quad (2.4)$$

This gives $\sigma_0^2 = \xi(0) = \langle V^2 \rangle$.

We can differentiate equation (2.3) and then set $\vec{\phi}_1 = \vec{\phi}_2$ to get

$$\begin{aligned} \langle \eta_i \eta_j \rangle &= \frac{1}{(2\pi)^N} \frac{\partial}{\partial \phi_1^i} \frac{\partial}{\partial \phi_2^j} \int d^N k e^{i\vec{k} \cdot (\vec{\phi}_1 - \vec{\phi}_2)} P(k) \Big|_{\vec{\phi}_1 = \vec{\phi}_2} \\ &= \frac{1}{(2\pi)^N} \int d^N k (k^i k^j) P(k) \end{aligned}$$

The integrand on the RHS is an odd function of both k^i and k^j , therefore the integral over all \vec{k} is zero unless $i = j$. Furthermore, because $k^2 = \sum_i k_i^2$, we see that $\sum_i \langle \eta_i \eta_i \rangle = \sigma_1^2$. We have assumed the field is statistically isotropic and thus $\langle \eta_i \eta_i \rangle = \langle \eta_j \eta_j \rangle$, meaning $\langle \eta_i \eta_i \rangle = \sigma_1^2/N$. Therefore $\langle \eta_i \eta_j \rangle = \delta_{ij} \sigma_1^2/N$.

A similar analysis holds for the second derivatives ζ_{ij} , which can be used to find the rest of the elements of the covariance matrix. In terms of the moments of the power spectrum they are:

² $\langle V \rangle = 0$ can always be obtained by a constant shift in the definition of V . $\langle \eta \rangle = 0$ and $\langle \zeta \rangle = 0$ can be enforced by assuming V is statistically isotropic in field space. An interesting path for future work would be to examine our results without this assumption of statistical isotropy.

³We work in a field space basis where the field space metric is Euclidean.

$$\begin{aligned}
\langle VV \rangle &= \sigma_0^2 \\
\langle \eta_i \eta_j \rangle &= \frac{1}{N} \delta_{ij} \sigma_1^2 \\
\langle V \zeta_{ij} \rangle &= -\frac{1}{N} \delta_{ij} \sigma_1^2 \\
\langle \zeta_{ij} \zeta_{kl} \rangle &= \frac{1}{N(N+2)} \sigma_2^2 (\delta_{ij} \delta_{kl} + \delta_{il} \delta_{jk} + \delta_{ik} \delta_{jl})
\end{aligned} \tag{2.5}$$

For $N = 3$ this reduces to equation A1 of [38] (hereafter called BBKS).

This covariance matrix is far from diagonal. Therefore, instead of using V , η and ζ we wish to adopt a basis of variables that is as diagonal as possible. The η_i variables are already diagonal, as are the ζ_{ij} terms with $i \neq j$. The ζ_{ii} variables are correlated however, and in fact are also correlated to V . We look for a set of N linear combinations of these N variables that is diagonal. For this we choose

$$\begin{aligned}
x_1 &= -\frac{1}{\sigma_2} \sum_i \zeta_{ii} \\
x_n &= -\frac{1}{\sigma_2} \sum_{i=1}^{n-1} \zeta_{ii} - (n-1) \zeta_{nn}, \quad (2 \leq n \leq N)
\end{aligned}$$

The x_n here are analogous, but not identical, to BBKS's x, y, z . Following BBKS, we also **rescale V and** introduce $\nu = V/\sigma_0$. With this choice of basis, the **new** nonzero correlations are, from equation (2.5):

$$\begin{aligned}
\langle \nu^2 \rangle &= 1 \\
\langle x_1^2 \rangle &= 1 \\
\langle \nu x_1 \rangle &= \gamma \\
\langle x_n^2 \rangle &= \frac{2n(n-1)}{N(N+2)}, \quad (2 \leq n \leq N)
\end{aligned} \tag{2.6}$$

where $\gamma = \sigma_1^2/(\sigma_2 \sigma_0)$. The only non-diagonal correlation left is between ν and x_1 .

The Q factor in equation (2.1) **can now be calculated and** takes the form

$$2Q = \nu^2 + \frac{(x_1 - \gamma \nu)^2}{1 - \gamma^2} + \sum_{n=2}^N \frac{N(N+2)}{2n(n-1)} x_n^2 + \frac{N \boldsymbol{\eta} \cdot \boldsymbol{\eta}}{\sigma_1^2} + \sum_{i,j;i>j}^N \frac{N(N+2)(\zeta_{ij})^2}{\sigma_2^2} \tag{2.7}$$

This is the equivalent of BBKS equation (A4) for N -dimensions, **and our slightly different definition of the x_n variables**. Note the first two terms remain constant for all N , but the remaining terms vary. The η terms are zero at minima by definition.

[**SH: I think this bit of the paragraph is not explained well**]while the off-diagonal ζ_{ij} terms can be Euler-rotated away by choosing an appropriate set of axes [**SH: I don't**

know what this means.]. The ξ matrix is already symmetric (by rotational symmetry), and Euler rotation turns it diagonal.[39]

The upshot is that ζ becomes diagonal and the individual elements of ζ are the eigenvalues $\lambda_i = -\zeta_{ii}$ of the Hessian. We are interested in minima, hence we demand all second derivatives to be positive, i.e. all eigenvalues to be **negative**.⁴ From here, the analysis is exactly the same as BBKS, except that when we define the ordering of the eigenvalues $\lambda_1 \leq \lambda_2 \leq \lambda_3 \dots \leq 0$, our boundary conditions become $x_1 \leq x_N \leq x_{N-1} \dots \leq x_2 \leq 0$ because of the different choice of **variables**. This leads to significantly simpler boundary conditions, for example in 3D our conditions are $x_1 \leq x_3 \leq x_2 \leq 0$ (compare BBKS's equation between Eq. (A14) and Eq. (A15)).

This yields the following expression for the **number** density of **minima**:

$$N_{peak} = A \int_{\lambda_1 \leq \lambda_2 \leq \lambda_3 \dots \leq 0} G \times e^{-Q} d\nu dx_1 dx_2 dx_3 \dots \quad (2.8)$$

where G has the form⁵[**SH: We haven't explained at all where G comes from. The rest is self-contained.**]

$$G = \left(\prod_i^N \lambda_i \right) \left(\prod_{i < j} |\lambda_i - \lambda_j| \right), \quad (2.9)$$

Q is given by Eq. 2.7, A is a constant factor, and the integration limits are only over the region where the conditions are satisfied. **We extract probabilities from this expression by calculating the proportion of minima satisfying various properties, hence we do not need to determine A explicitly because it cancels when we take ratios to determine proportions.** Evaluating this integral will be the focus of much of the remainder of this paper.

3 Peak Probabilities: V and N

Our goal is to evaluate $P(V|min)$ for Gaussian random landscape potentials, the probability density that defines the distribution of vacuum energies at minima in the landscape. We are interested in the probability of finding a minimum above $\nu = 0$ (equivalently, the probability of finding a maximum below $\nu = 0$), i.e. we want to calculate

$$P(V|min) = \frac{\int_0^\infty d\nu \int_{\lambda_1 \geq \lambda_2 \geq \lambda_3 \dots \geq 0} G \times e^{-Q} dx_1 \dots dx_N}{\int_{-\infty}^\infty d\nu \int_{\lambda_1 \geq \lambda_2 \geq \lambda_3 \dots \geq 0} G \times e^{-Q} dx_1 \dots dx_N} \quad (3.1)$$

This integral depends on the value of Q (Eq. 2.7) and therefore on the moments of the power spectrum σ_0, σ_1 , and σ_2 . We now argue that of these three parameters, only one is physically significant. Given a purely Gaussian landscape we can $\sigma_0 = 1$ by rescaling V multiplicatively, see Eq. 2.5, and we can thus take $F = \nu$. Likewise,

⁴Note there is an alternative convention where the eigenvalues **are defined with the opposite sign, in which case positive eigenvalues** correspond to **minima**

⁵ G can also be expressed in terms of x_i using the inverse transform of Eq. ??

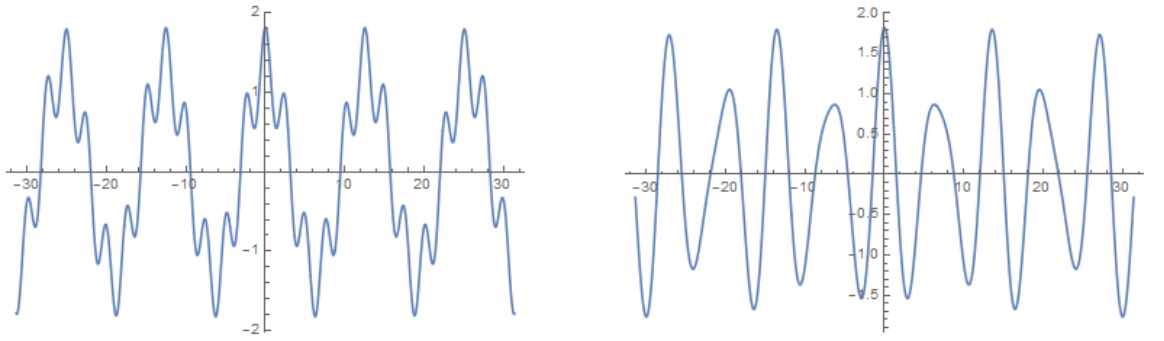


Figure 1. We show illustrative realisations of 1D functions. The left figure has a smaller γ (larger σ_2) and more “short scale” power, allowing minima (maxima) to appear in significant numbers above (below) zero. When γ is large (right figure) the spectrum is dominated by longer wavelength modes, and most minima are low-lying.

σ_1 responds to the average magnitude of the first derivatives and can be set to unity by rescaling the units of length. This leaves σ_2 as the only nontrivial parameter. It can be shown that if $\sigma_0 = \sigma_1 = 1$, $\sigma_2 > 1$.⁶ In much of what follows we follow BBKS and parameterise the landscape by $\gamma = \frac{\sigma_1^2}{\sigma_2 \sigma_0} = 1/\sigma_2$ and the dimensionality N , in the knowledge that $0 < \gamma < 1$.

3.1 Landscape Heuristics

We begin by making a qualitative exploration of the overall “likelihood”. Firstly, we note that the integrand vanishes when any two “adjacent” λ_i become equal, enforcing an “eigenvalue repulsion” in the Hessian matrices for the maxima and minima. This implies that a generic minima will be asymmetric, as their Hessians will have well separated eigenvalues.

Secondly, looking at Eq. 2.7 we see that if γ is close to unity, the second term in Q becomes very large, making the integrand a steeper function of the x_i . Conversely, if γ is small, ν can take larger values without dominating Q . At larger values of γ the power spectrum is effectively “red” and the random function is dominated by longer wavelength modes. By contrast, when γ is small the spectrum is “blue” and dominated by shorter modes. In this case, it is more likely that extrema will be found at positive values of ν . This behaviour is sketched in Fig 1 for illustrative one dimensional examples.

Thirdly, as N increases Q will always grow, making it less likely to find minima and maxima on the “wrong” side of zero.

Finally, because we are interested in the regimes $\nu = 0 \dots \infty$ and $\nu = -\infty \dots \infty$, we can simplify the integral Eq. 3.1 by performing the ν integral analytically. The only dependence in the integrand on ν is in the first two terms of Q , which further remains the same for all N :

⁶Per Ref. [21], if $\sigma_0 \sigma_2 - \sigma_1^2 < 0$, then the probability density Eq. ?? cannot be normalized.

$$\begin{aligned}
& \int_{-\infty}^{\infty} d\nu \int_{\lambda_1 \geq \lambda_2 \geq \lambda_3 \dots \geq 0} G \times e^{-Q} dx_1 \dots dx_N \\
&= \int_{-\infty}^{\infty} d\nu e^{-\frac{\nu^2}{2} - \frac{(x-\gamma\nu)^2}{2(1-\gamma^2)}} \int_{\lambda_1 \geq \lambda_2 \geq \lambda_3 \dots \geq 0} f(x_1, x_2 \dots) dx_1 \dots dx_N \\
&= \int_{-\infty}^{\infty} d\nu e^{-\frac{x^2}{2} - \frac{(\nu-\gamma x)^2}{2(1-\gamma^2)}} \int_{\lambda_1 \geq \lambda_2 \geq \lambda_3 \dots \geq 0} f(x_1, x_2 \dots) dx_1 \dots dx_N \\
&= e^{-\frac{x^2}{2}} \sqrt{2\pi} \sqrt{1-\gamma^2} \int_{\lambda_1 \geq \lambda_2 \geq \lambda_3 \dots \geq 0} f(x_1, x_2 \dots) dx_1 \dots dx_N
\end{aligned} \tag{3.2}$$

Similarly,

$$\begin{aligned}
& \int_0^{\infty} d\nu \int_{\lambda_1 \geq \lambda_2 \geq \lambda_3 \dots \geq 0} G \times e^{-Q} dx_1 \dots dx_N \\
&= e^{-\frac{x^2}{2}} \sqrt{\frac{\pi}{2}} \sqrt{1-\gamma^2} (1 + \text{Erf}(\frac{\gamma x}{\sqrt{2-2\gamma^2}})) \int_{\lambda_1 \geq \lambda_2 \geq \lambda_3 \dots \geq 0} f(x_1, x_2 \dots) dx_1 \dots dx_N
\end{aligned} \tag{3.3}$$

Although these analytic integrals are not always usable in what follows, when they are, they lighten the computational cost significantly.

3.2 $N < 10$: Direct Evaluation

For relatively small values of N we can compute the integrals without any further approximations. In Figs. 2 and 3, we present $P(F > 0|min)$ as a function of N and γ . As expected, if the potential is highly oscillatory (σ_2 large, or γ small), $P(F > 0|min)$ tends towards 0.5 – an equal likelihood of any given extremum being a maximum or a minimum. Conversely, if the potential is very smooth (σ_2 small; γ very large), $P(F > 0|min)$ tends towards 0. Moreover, for any given γ , $P(F > 0|min)$ decreases with increasing N .

3.3 $10 < N < \sim 30$: Gaussian Approximations to the Integral

For $N > 10$, direct calculation becomes very resource-intensive. To proceed, we first select a value of the field ν , then find the values of $x_1, x_2 \dots$ that maximizes the integral in in Eq. 2.8. We then approximate the integral as a Gaussian integral about this maximum likelihood point:

$$\begin{aligned}
N &= A \int_{\lambda_1 \geq \lambda_2 \geq \lambda_3 \dots \geq 0} F \times e^{-Q} dx dy dz \dots \\
&= A \int_{\lambda_1 \geq \lambda_2 \geq \lambda_3 \dots \geq 0} e^{\log F - Q} dx dy dz \dots \\
&\approx \int_{-\infty}^{\infty} e^{-\frac{1}{2} x H x} d^n x = \sqrt{\frac{(2\pi)^n}{\det H}}
\end{aligned}$$

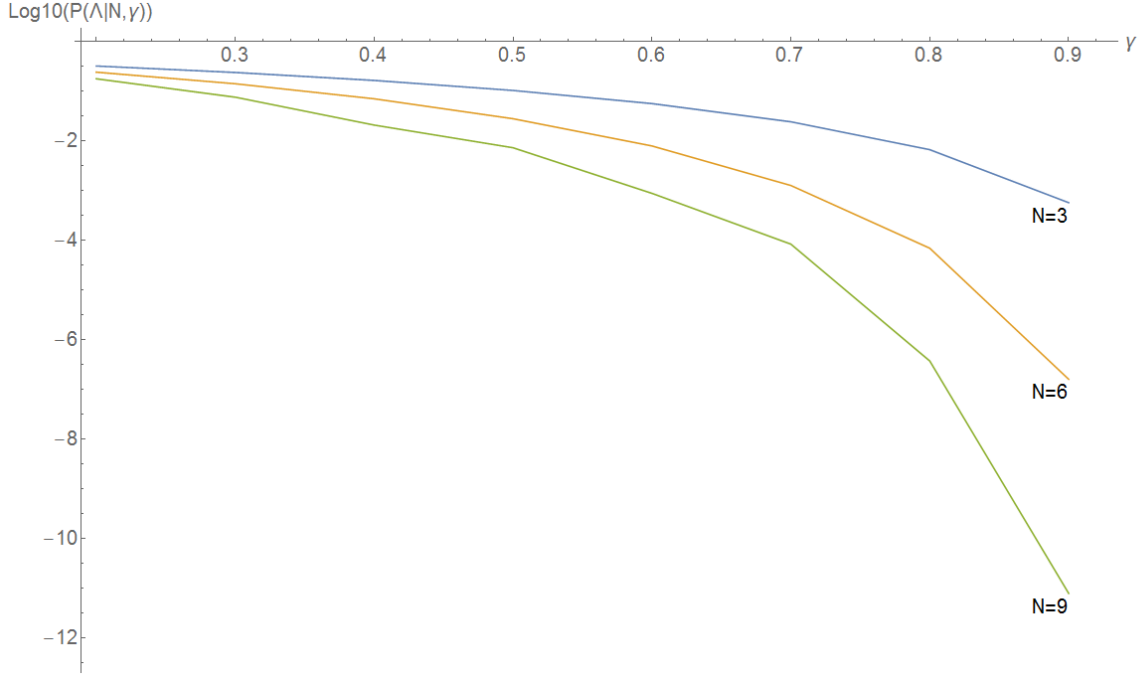


Figure 2. The probability that a given minimum has $F > 0$ as a function of γ , for $N = 3, 6, 9$. We can see that all the heuristics are obeyed: the probability decreases with N , and increases with σ_2 . [RE: gamma? Also – we can smooth this, and use the LogListPlot (or ListLogPlot, or whatever it is) command in mathematica]

where H is the Hessian at the point being considered, and we no longer have an integral over ν . This produces a list of points for each value of ν . Fitting these points to a function and integrating that for the region with $\nu > 0$, we get an approximate result of the integral. [LL: I feel like there's a more technical term for this, don't know what though.] This approximate value can then be compared against the exact value. The Gaussian approximation turns out to be very good (see Fig. 5). The Gaussian integral can be more efficiently computed than Eq. 2.8, which lets us evaluate it up to $N \approx 30$.

The plot of the logarithms of these results against the number of dimensions is surprisingly straight (Fig. 6). Although it is not conclusive,⁷ it is suggestive.

3.4 $\sim 30 < N < \sim 100$: Approximations using the $\nu = 0$ point

The Gaussian approximation described in the previous subsection requires the integral to be computed for several different values of ν . If we use only the result at the $\nu = 0$ point, we get a result that is much larger than the exact results, but it remains at a nearly-constant ratio to it (see Fig. 4). Using this, we confirm that the straight line behavior holds up to $N = 100$.

Based on these calculations, we conclude that the value of σ_2 for which $P(F > 0|min)$ drops to $\sim 10^{-500}$ at $N = 100$ is about 1.08. In other words, there will be plenty

⁷Per Figure 4 of [21], it is possible the behavior of the function changes at $N > 100$.

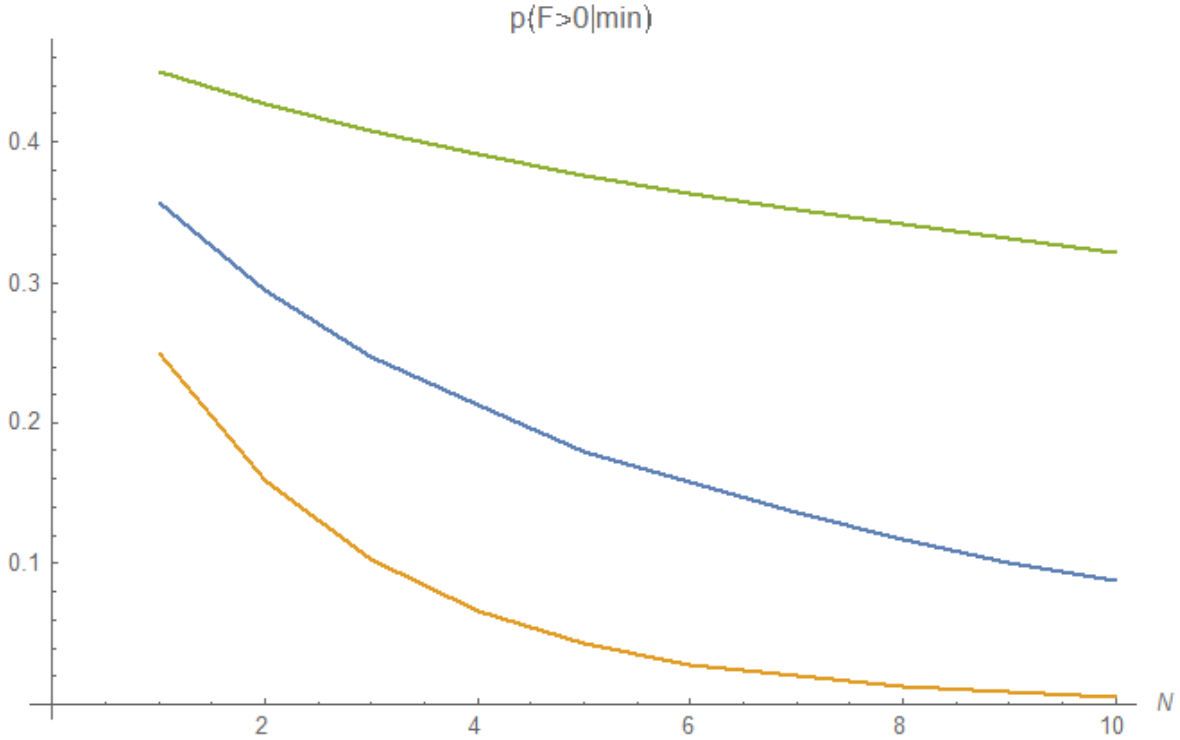


Figure 3. A plot showing the value of $P(F > 0|min)$ as a function of N with $N \leq 10$, for γ values $\frac{1}{5}$, $\frac{1}{3.5}$ and $\frac{1}{2}$ from top to bottom.

of minima in the landscape that could correspond to our universe if the landscape has $\sigma_2 \gtrsim 1.08$ (with σ_0 and σ_1 normalized to 1).

4 Implications for Multiverse Cosmology

[RE: I would move from looking at the abstract problem in the previous section to the specific implications for cosmology in this section; and how $P(\Lambda)$ depends on σ_2]

[LL: Dunno what to put here anymore]

5 Conclusion

We have presented results for the statistics of stationary points at a given function value as a function of N and σ_2 . The numbers confirm the intuitive expectation that the probability of a given extremum with $F > 0$ being a minimum decreases as N increases or as σ_2 decreases. We are able to calculate precise values for the probability up to $N = 10$. Above this dimension, evaluating Eq. 2.8 is computationally prohibitive, but we find that Eq. 2.8 is well-approximated by a Gaussian integral. Using this approximation, we are able to estimate the probability up to $N \approx 30$. For $N > 30$, we use only the $\nu = 0$ point, which although much smaller than the actual results, remains in roughly constant ratio with it. The final probability as a function of N is

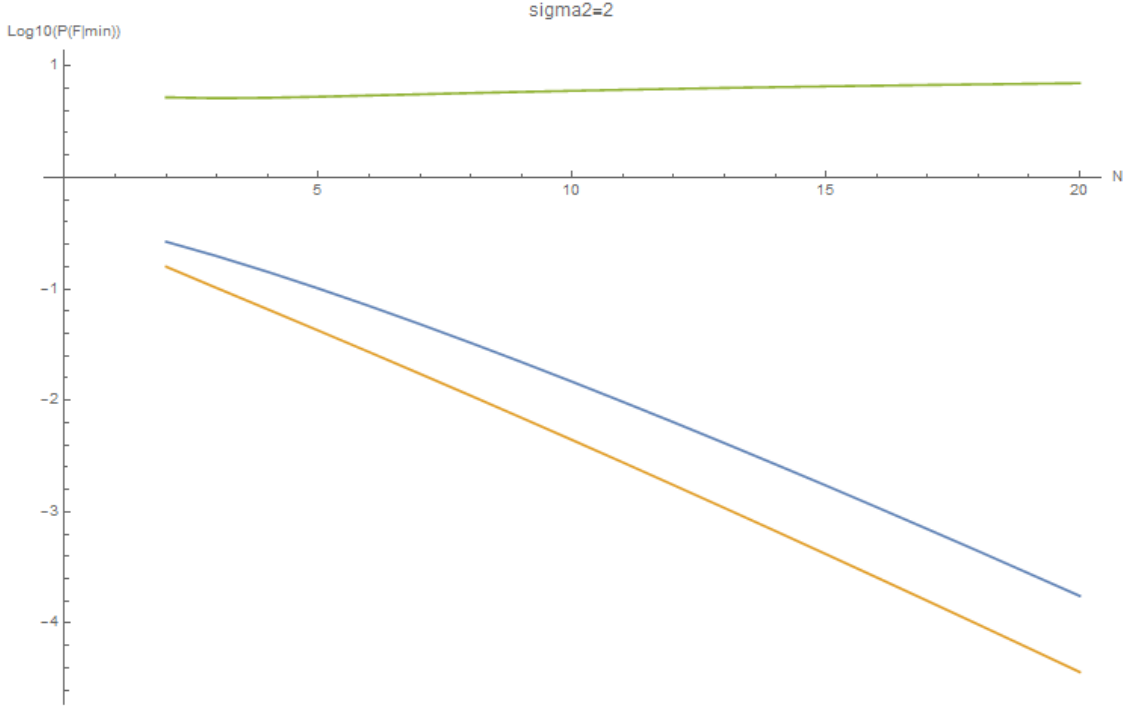


Figure 4. A comparison of the Gaussian approximation evaluated at the $\nu = 0$ point to the full integral. The blue line corresponds to the $\nu = 0$ results, while the orange line corresponds to the Gaussian results (Section 3.3). Horizontal axis is N while the vertical axis is the Log_{10} of the probability. The $\nu = 0$ results are always larger than the actual results, but the ratio of their logarithms is approximately constant.

well-approximated by a straight line when plotted on a logarithmic scale for various values of σ_2 (Fig. 6). If this trend holds to larger values of N , we estimate that the value of σ_2 for which $P(F > 0|min)$ drops to $\sim 10^{-500}$ is approximately 1.08.

The results of this paper establish the number of vacua that could correspond to our universe in string theory, but does not treat the distribution of eigenvalues – and accordingly the duration of slow-roll inflation – that could arise from these vacua. An analysis of this will be the focus of future work.

6 Appendix

6.1 Density of peaks for $N = 4$

For $N = 4$, the full result of the integral Eq. 2.8 is: [LL: This needs to be re-checked, there shouldn't be x in the result. Computer is busy with the $N = 100$ calculations for $\sigma_2 = 1.08$, will do it later.]

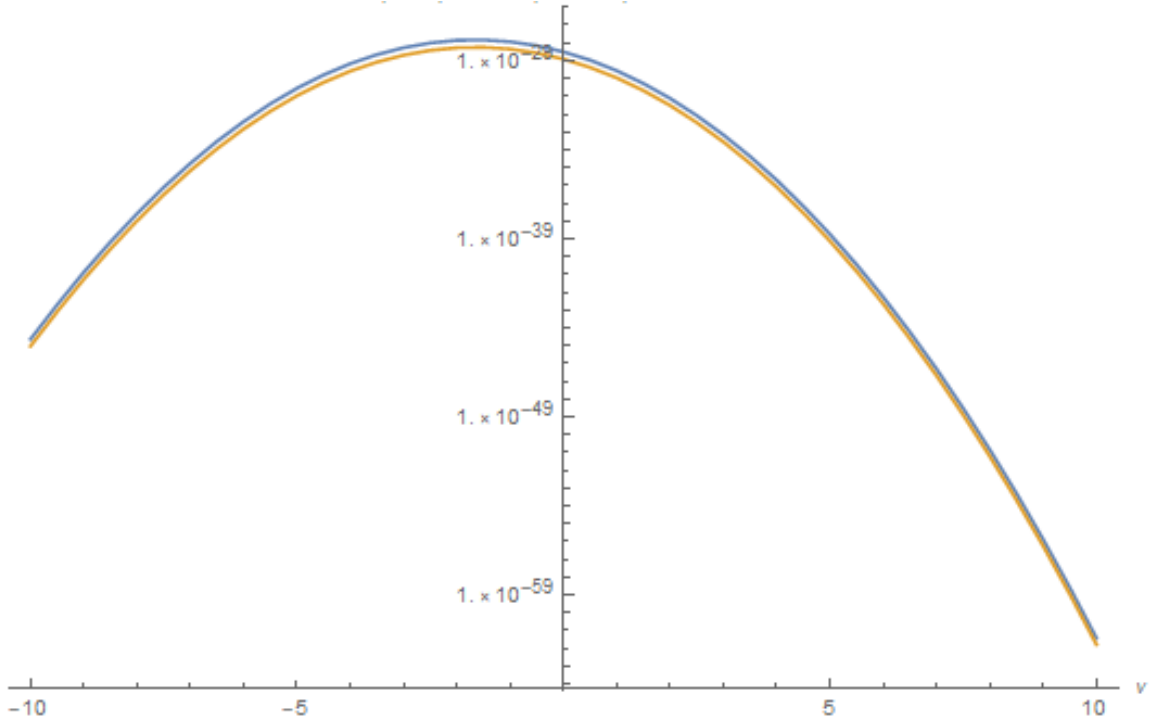


Figure 5. A comparison of $P(F)$ with the Gaussian approximation, at specified values of ν ($N = 8$). Blue line corresponds to the Gaussian results, while the orange line corresponds to the exact integral. Horizontal axis is ν while the vertical axis is (unnormalized) likelihood. As expected, because the Gaussian integral integrates to infinity while the exact integral does not, it yields a larger likelihood.

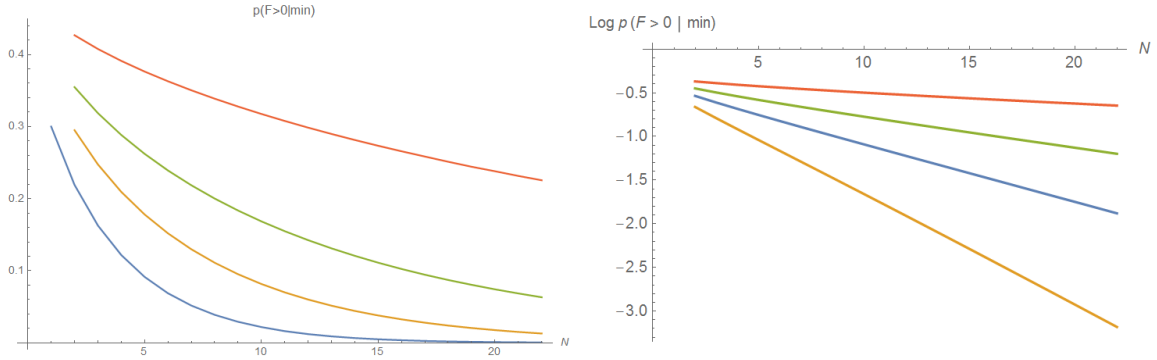


Figure 6. (Left) The probability of a minimum above $\nu = 0$, calculated using the Gaussian approximation. The lines correspond to $\gamma = \frac{1}{10}, \frac{1}{5}, \frac{1}{3.5}, \frac{1}{2.5}$ respectively from top to bottom. Compare Fig. 3. (Right) The same data, plotted using a different y-axis (Log here is to base 10). All four lines yield a logarithm well above -500 at $N = 100$. The cutoff at which $p(F > 0 | \min) \sim 10^{-500}$, with σ_0 and σ_1 normalized to 1, is $\sigma_2 \approx 1.08$.

$$N = \frac{1}{214990848} \text{Exp} \frac{9x^2\sigma_1^4 + 2\nu x\sigma_0\sigma_1^2\sigma_2 - (v^2 + 10x^2)\sigma_0^2\sigma_2^2}{-2\sigma_1^4 + 2\sigma_0^2\sigma_2^2} \quad (6.1)$$

$$\left(80x - 1610e^{\frac{9x^2}{2}} + 128x^3 + 418e^{\frac{9x^2}{2}}x^3 + 4e^{\frac{9x^2}{2}}\sqrt{\pi}(3 + 48x^2 + 64x^4)\text{Erf}\left[\sqrt{\frac{3}{2}}x\right] \right. \\ \left. - 486e^{\frac{9x^2}{2}}\sqrt{6\pi}x^2\text{Erf}\left[\sqrt{\frac{3}{2}}x\right] + 81e^{\frac{9x^2}{2}}\sqrt{6\pi}x^4\text{Erf}\left[\sqrt{\frac{3}{2}}x\right] \right)$$

The higher-dimensional results take the same form: an overall exponential multiplied by a product of polynomials and error functions; however they are massive (for example, in 5D there are some eight hundred terms).

6.2 $p(F|s.p.)$ for $N = 2$

[LL: As long as the reference above to the difference with Yamada & Vilenkin is commented out, this appendix isn't needed either] The full expression for $p(F|s.p.)$ in 2D is:

$$p(F|s.p.) = \frac{\sqrt{\pi}}{4\sqrt{4\gamma^2 - 6}} \left[\text{Exp} \frac{F^2}{2(\gamma^2 - 1)} \left(2\text{Exp} \left(\frac{F^2\gamma^2}{e^6 - 10\gamma^2 + 4\gamma^4} \right) \sqrt{\gamma^2 - 1} \right. \right. \\ \left. \left. - \text{Exp} \left(\frac{F^2\gamma^2}{2 - 2\gamma^2} \right) (F^2 - 1)(\gamma^2 - 1)\gamma^2 \sqrt{\frac{2\gamma^2 - 3}{1 - \gamma^2}} \right) \right] \quad (6.2)$$

where $\gamma = \sigma_1^2/\sigma_0\sigma_2$. This result can be derived using a similar method as to derive Eq. 2.8, but by relaxing the requirement that the smallest eigenvalue is greater than zero.

References

- [1] Planck Collaboration 2018 results. Submitted to *Astronomy & Astrophysics*.
- [2] Dark Energy Survey year 1 results. arXiv:1802.05257
- [3] A. D. Linde, Phys. Lett. B 175, 4, 395–400, 1986
- [4] P. Adshead, R. Easther, and E. A. Lim, Phys. Rev. D 79, 063504, 2009
- [5] A. Guth, arXiv: astro-ph/0101507
- [6] L. Susskind, arXiv:hep-th/0302219
- [7] R. Bousso and J. Polchinski, Journal of High Energy Physics, 06, 006, 2000
- [8] P. Agrawal, G. Obied, P. J. Steinhardt, C. Vafa, Physics Letters B, 784, 271–276, 2018
- [9] A. Masoumi, A. Vilenkin and M. Yamada, Journal of Cosmology and Astroparticle Physics, 05:053, 2017
- [10] A. Masoumi, A. Vilenkin and M. Yamada, Journal of Cosmology and Astroparticle Physics, 12:035, 2017
- [11] T. Bjorkmo and M.C.D. Marsh, Journal of Cosmology and Astroparticle Physics, 02:037, 2018
- [12] A. Aazami and R. Easther, Journal of Cosmology and Astroparticle Physics (0603:013), 2006
- [13] A. J. Bray and D. S. Dean, Physical Review Letters, 98, 150201, 2007
- [14] R. Easther and L. McAllister, Journal of Cosmology and Astroparticle Physics 05:018, 2006

- [15] J. Frazer and A. R. Liddle, *Journal of Cosmology and Astroparticle Physics* 02:026, 2011
- [16] S.-H. Henry Tye, J. J. Xu and Y. Zhang, *Journal of Cosmology and Astroparticle Physics* 04:018, 2009
- [17] M.C.D. Marsh, L. McAllister, E. Pajer and T. Wrase, *Journal of Cosmology and Astroparticle Physics* 11:040, 2013
- [18] N. Agarwal, R. Bean, L. McAllister and G. Xu, *Journal of Cosmology and Astroparticle Physics* 09:002, 2011
- [19] I.S. Yang, *Physical Review D*, 86, 103537, 2012
- [20] A. Masoumi and A. Vilenkin, *Journal of Cosmology and Astroparticle Physics* 03:054, 2016
- [21] M. Yamada and A. Vilenkin, *Journal of High Energy Physics* 2018: 29, 2018
- [22] Y. V. Fyodorov, *Physical Review Letters*, 92, 240601, 2004
- [23] M. R. Douglas, B. Shiffman and S. Zelditch, *Communications in Mathematical Physics*, 252, 325, 2004
- [24] M. R. Douglas, B. Shiffman and S. Zelditch, *Communications in Mathematical Physics*, 265, 617, 2006
- [25] Y. V. Fyodorov and I. Williams, *Journal of Statistical Physics*, 129, 5, 2007
- [26] Y. V. Fyodorov and C. Nadal, *Physical Review Letters*, 109, 167203, 2012
- [27] Y. V. Fyodorov, P. L. Doussal, A. Rosso, C. Texier, *Annals of Physics*, 397, 2018
- [28] V. Ros, G. B. Arous, G. Biroli and C. Cammarota, *Physical Review X* 9, 011003
- [29] D. S. Dean and S. N. Majumdar, *Physical Review E*, 77, 041108, 2008
- [30] S. N. Majumdar, C. Nadal, A. Scardicchio, and P. Vivo., *Physical Review Letters*, 103, 220603, 2009
- [31] T.C. Bachlechner, *Journal of High Energy Physics*, 2014: 54, 2014
- [32] D. Battefeld, T. Battefeld, S. Schulz, *Journal of Cosmology and Astroparticle Physics*, 06:034, 2012
- [33] Y. V. Fyodorov, *Markov Processes Relat. Fields*, 21, 483–51, 2015
- [34] A. Masoumi, M. Yamada and A. Vilenkin, *Journal of Cosmology and Astroparticle Physics*, 07:003, 2017
- [35] R. Easther, A. Guth and A. Masoumi, *arXiv:1612.05224* (2016)
- [36] M. Kac, *Bull. Amer. Math. Soc.*, 43, 314–320, 1943
- [37] S. O. Rice, *Bell System Tech. J.*, 24, 46–156, 1945
- [38] J. M. Bardeen, J. R. Bond, N. Kaiser, and A. S. Szalay, *Astrophysical Journal*, *Astrophysical Journal*, vol. 304, page 15-61 (1986)
- [39] See e.g. H. Goldstein, C. P. Poole, and J. L. Safko, *Classical Mechanics 3rd ed.*, Pearson (2001)
- [40] G. P. Lepage, *Journal of Computational Physics* 27, 192, 1978.

- [41] B. Gough, *GNU Scientific Library Reference Manual - Third Edition, 3rd ed.* (Network Theory Ltd., 2009).
- [42] M. R. Douglas, Journal of High Energy Physics, 05:046, 2003